NASA-TM-75862 19800024838

NASA TECHNICAL MEMORANDUM NASA TM-75862

ON THE SWELLING OF ROLLED UP VORTEX SURFACES AND THE BREAKDOWN OF THE VORTEX CORE FOR SLENDER WINGS

Arabindo Das

Translation of "Zum Anschwellen aufgerollter Wirbelflächen und Aufplatzen des Wirbelkerns bei schlanken Tragflügeln", Z. Flugwiss. 15(1967), pp 355-362

NATIONAL AERONAUTICS AND SPACE ADMINISTRATION
WASHINGTON D.C. 20546 OCTOBER 1980

STANDARD TITLE PAGE

1. Report No. NASA TM-75862	2. Government Accession No.	3. Recipient's Catalog No.
4. Title and Subtitle ON THE SWELLING OF ROLLED UP VORTEX SURFACES AND THE BREAKDOWN OF THE VORTEX CORE FOR SLENDER WINGS.		5. Report Date OCTOBER 1980 6. Performing Organization Code
7. Author(s) Arabindo Das		8. Performing Organization Report No. 10. Work Unit No.
9. Performing Organization Name and Address SCITRAN Box 5456 Santa Barbara, CA 93108		11. Contract or Grant No. NASW-3198 13. Type of Report and Period Covered Translation
12. Sponsoring Agency Name and Address National Aeronautics and Space Administration Washington, D.C. 20546		14. Sponsoring Agency Code

15. Supplementary Notes

Translation of "Zum Anschwellen aufgerollter Wirbelflächen und Aufplatzen des Wirbelkerns bei schlanken Tragflügeln", Z. Flugwiss. 15(1967), pp 355-362

16. Abstract The rolled-up vortex sheet of a slender wing often displays an instability which manifests itself by a sudden swelling of the cylindrical vortex surface and a bursting of the vortex core. As known experimentally, the longitudinal distribution of vortices of the rolledup sheet can be subjected to a reduction of strength as well as to a reversal of the sense of rotation of the vortices. These processes can be simulated by simplified models of the vortex distribution over cylindrical surfaces. The effect of such a change of vortex strength has been analyzed quantitatively by means of potential theory. The results illustrate the considerable bulging of the cylindrical vortex sheet as a consequence of the change of the vortex strength. The coiling-up of the vortices rotation in opposite directions over the cylindrical surface renders the condition for instability and the subsequent large spreading of the vortex core. These processes occur without a positive pressure gradient being necessary in the field of flow surrounding the coiled up vortex sheet.

17. Key Words (Selected by Author(s))	18. Distribution Statement
	Unclassified - Unlimited

19. Security Classif. (of this report)	20. Security Classif. (of this page)	21. No. of Pages	22.
Unclassified	Unclassified	26	

ON THE SWELLING OF ROLLED UP VORTEX SURFACES AND THE BREAKDOWN OF THE VORTEX CORE FOR SLENDER WINGS

Arabindo Das

1. Introduction

/356*

The rolling up of vortex braids at the free ends of wings is a familiar phenomenon. Its origin can be traced back to the difference in pressure between the lower and upper sides of the wing and the circulatory flow around the free ends which this pressure gradient calls forth.

In slender delta wings, in which the leading edge also takes over the role of the side edges, an oblique circulatory flow around this edge appears. However, the current cannot flow adjacently around the abrupt leading edge, because with the appearance of circulatory flow velocities, the radial pressure force necessary for equilibrium does not come about. This fact may be understood by recognizing that the buildup of the necessary radial velocity gradients is hindered by the viscosity of the air. Further, an abrupt pressure increase from the edge to the middle of the wing arises with the circulatory flow around the slender wing. Because of the appearance of the viscous force in the circulating flow, the current cannot overcome this pressure gradient. Consequently, the flow detaches from the edge and produces a rolled up vortex surface. The spiral forming free vortices, which are depicted in Fig. 1, form the requisite continuation of the bound vortices of the wing surface.

*Numbers in the margin indicate pagination in the foreign text.

The manner of coiling of the vortex surface for a slender wing has been described in the papers [1 to 3]. A physical representation of the particulars of the flow for such rolled up vortex surfaces was given by M. Roy [4]. The theoretical determination of the flow field of a conically coiled vortex surface was treated by R. Legendre [5]. Further, the position and form of the coiled vortex surface of a slender delta wing was theoretically calculated by J. H. B. Smith [6]. Extensive experimental investigations in the region of the rolled up vortex were carried out by N. C. Lambourne and O. W. Bryer [7], P. T. Fink [8] and D. Hummel [9, 10].

It has been variously observed that the rolled up vortex surface shows an instability under certain conditions. The instability manifests itself through a sudden swelling of the vortex surface [1,2]. This phenomenon is often designated as breakdown of the vortex. Detailed experimental investigations of the manner and cause of breakdown of the vortex were undertaken in [9 to 14] in order to gain knowledge about the physical processes involved in the breakdown of a vortex. Also, some theoretical papers [15 to 19] were produced in order to clarify this phenomenon of breakdown of a vortex, However, these papers give no completely satisfactory solution to this phenomenon.

A stability theory for helical vortices in cylindrical ring space was developed by J. Ludwieg [20] and experimentally proven [21]. This theory was then carried over to the case of the coiled vortex sheet for slender wings. Two other publications of H. Ludwieg [22,23] contributed to the further clarification of the breakdown of vortex cores.

To confirm the instability criterion which was asserted by H. Ludwieg [22] for spiral vortices in the rolled up vortex

sheet of a slender wing, D. Hummel [9,10] undertook detailed experimental investigations. He was able to prove that this instability criterion was also valid for such a vortex sheet although the actual flow model differed considerably from the greatly idealized flow model of H. Ludwieg. A summary of these theoretical and experimental papers has been given by H. Schlichting in [24].

The stability investigations which have been carried out give no complete insight into either the propagation of the breakdown position upstream with increasing attack angle or the sudden appearance of a large pressure gradient in the free vortex sheet. Such a pressure gradient is necessary for the breakdown. In the present paper, as a contribution to the clarification of these questions, the swelling of a cylindrical vortex sheet will be quantitatively investigated for various conditions.

2. Explanation of symbols (compare Fig. 1 and Fig. 3)

2.1 Geometric quantites

R	radius of the cylindrical vortex sheet
r	radial distance
x,y,z	cartesian coordinates
ξ	dimensionless distance (=x/R)
ψ	angular coordinate
ω	inclination angle of the spiral forming vortices

2.2 Aerodynamic quantities

V_∞	incident flow velocity
Γ	circulation
χ	vortex density $(=\partial\Gamma/\partial x$ or $\partial\Gamma/\partial\tau)$
u, v_r, v_ψ	induced velocities.

3. Calculation of the induced velocity field of a cylindrical vortex surface

The manner of coiling of a vortex sheet of a slender delta wing is illustrated in Fig. 1. The free vortices with strength $\Delta\Gamma\omega$, which arise on the leading edge of a wing, have a helical development. The inclination angle of these helical vortices follows from the condition that the vortex lines develop parallel to the resulting flow direction so that no forces can originate on the free vortex lines.

These helical vortices quickly coil up in a spiral like fashion (Fig. 2a). A vortex core forms in the center of the spiral forming vortex. All free vortices arising on the leading edge of the wing spiral into the vortex core and progress downstream. Consequently, the strength of the vortex core increases with tip length and achieves its maximum value at the trailing edge of the wing.

/357

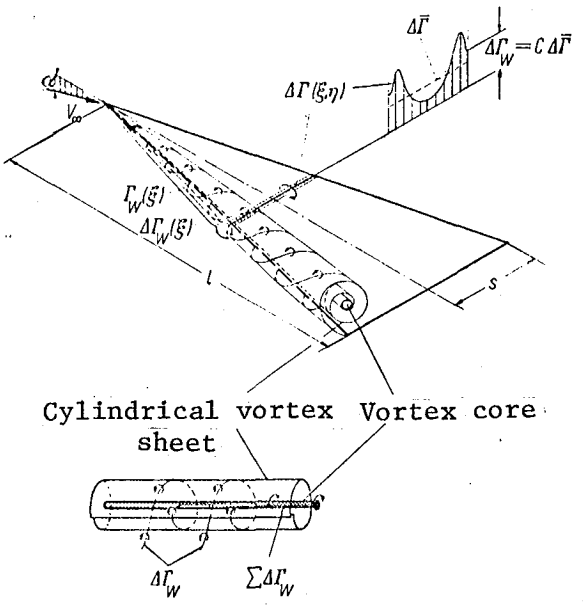

Fig. 1 The origin of a rolled up vortex surface for a slender wing.

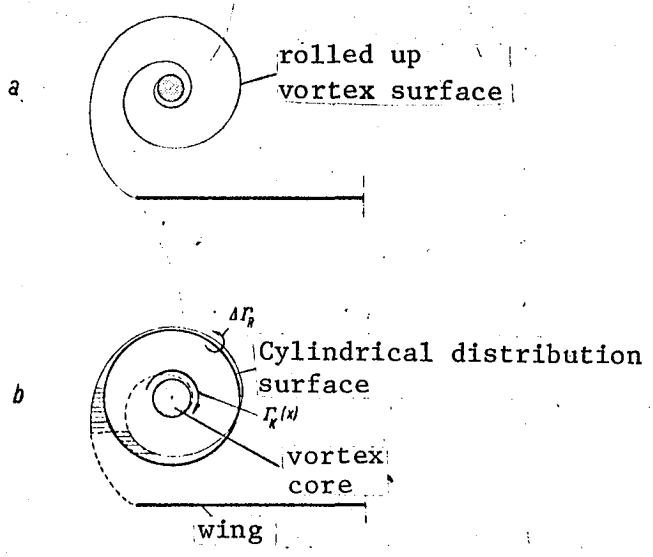

Fig. 2 Idealization of the rolled up vortex surface by a sliced cylindrical distribution surface and a vortex core.

To simplify the vortex model, the rolled up vortex surface can be replaced by a longitudinally sliced cylindrical vortex distribution surface and a vortex core (Fig. 2b). The vortices progress further helically and spirallike. This model of the cylindrical distribution surface represents a mathematical simplification corresponding to the vortex distribution on the chord of a wing profile. It is different from the vortex model of H. Ludwieg [22] in that the entire coiled up vortex surface is considered as the core.

The assumption that the vortex surface of a slender wing elongated in the flow direction has a cylindrical character

corresponds to the assumption of the theory of slender wings according to which all changes in the geometrical and aerodynamic quantities take place very slowly in the flow direction.

While the spiral forming vortex lines produce induced velocities in all three directions on the cylindrical surface, the vortex core, which is directed along the axis direction, merely furnishes circulatory velocities in the surrounding field. Consequently, only the helical vortices on this surface are taken into consideration in the determination of the deformation of the cylindrical vortex surface.

The uniform distribution of the cylindrical vortex surface with spiral forming vortices can be constructed from a distribution of vortex rings of strength $\Delta\Gamma_R = \Delta\Gamma_W \cos\omega$ and a distribution of straight vortex filaments of strength $\Delta\Gamma_F = \Delta\Gamma_W \sin\omega$ in the longitudinal direction on the cylindrical surface (compare Fig. 3).

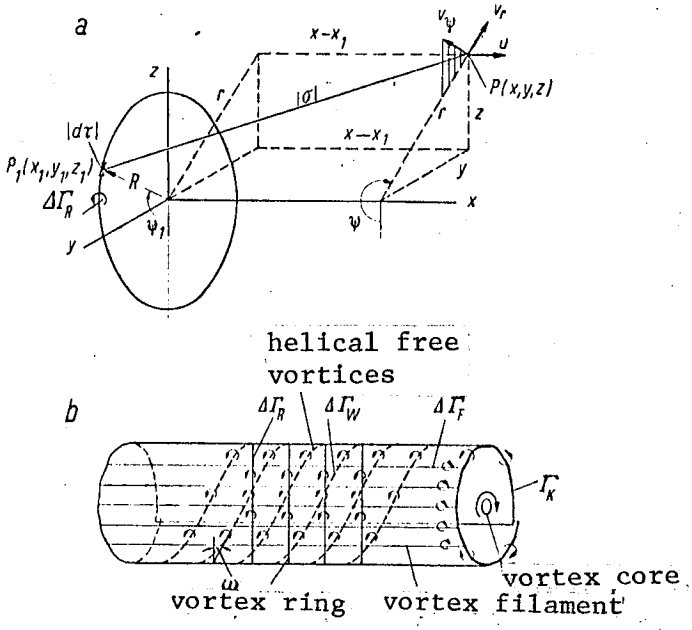

Fig. 3 The induced velocity of a vortex ring and a cylindrical vortex sheet with constant distribution of vortex rings.

The induced velocities of both parts can then easily be ascertained. The induced velocities of vortex filaments and vortex rings have been extensively treated in [25,26]. The application of vortex rings to ring wings and to cylindrical shrinking is found in [27,28].

To determine the induced velocities of a ring vortex on can apply the well known Biot-Savart law for a vortex element. According to Fig. 3, it reads

$$dw(x,y,z) = \frac{\Delta\Gamma}{4\pi}\frac{\sigma \cdot d\tau}{|\sigma|^3}, \tag{1}$$

where $|d\tau| = R\,d\psi_1$ denotes an element of the ring vortex and where

$$\begin{cases} \sigma = \mathbf{i}(x - x_1) + \mathbf{j}(r\sin\psi - R\sin\psi_1) + \\ \qquad + \mathbf{k}(r\cos\psi - R\cos\psi_1), \end{cases} \tag{2a}$$

$$\begin{cases} |\sigma| = [(x - x_1)^2 + r^2 + R^2 - \\ \qquad - 2rR\cos(\psi_1 - \psi)]^{1/2}, \end{cases} \tag{2b}$$

$$d\tau = R\,d\psi_1(\mathbf{j}\cos\psi_1 - \mathbf{k}\sin\psi_1) \tag{2c}$$

One can now integrate these elementary contributions around the ring vortex and separate the resulting induced velocity into radial and axial components. The radial velocity on the cylindrical vortex surface is found to satisfy the expression

$$\begin{cases} \dfrac{\Delta v_r(R, x - x_1)}{V_\infty} = \\ = \dfrac{R}{4\pi}\displaystyle\int_0^{2\pi} \frac{\Delta\Gamma_R(x_1)}{V_\infty}\frac{(x - x_1)\cos(\psi_1 - \psi)}{|\sigma|^3}\,d\psi_1 \end{cases} \tag{3}$$

with $\Delta\Gamma_R = \Delta\Gamma \cos\omega$, while for the axial velocity at r=R one has

$$\left\{ \begin{array}{l} \dfrac{\Delta u(R, x-x_1)}{V_\infty} = \\ = -\dfrac{R}{4\pi}\displaystyle\int_0^{2\pi} \dfrac{\Delta\Gamma_R(x_1)}{V_\infty} \dfrac{r\cos(\psi_1-\psi)-R}{|\sigma|^3}\, d\psi_1 . \end{array} \right. \qquad (4)$$

The distribution of the straight vortex filaments of the cylindrical vortex surface furnishes the circulatory velocity for r=R

$$\frac{v_\psi(R, x-x_1)}{V_\infty} = \frac{\Delta\Gamma_W \sin\omega}{V_\infty R\, d\psi_1} = \frac{\Delta\Gamma_F}{V_\infty R\, d\psi_1}. \qquad (5)$$

Equation (5) yields

$$\frac{v_\psi}{V_\infty} = \frac{\varkappa_F}{V_\infty}, \qquad (5a)$$

where $\varkappa_F = \partial\Gamma_F/\partial\tau$.

For the resulting radial velocity at r=R from the vortex rings of the entire cylindrical vortex sheet one has

$$\left\{ \begin{array}{l} \dfrac{v_r(R, x)}{V_\infty} = \dfrac{R}{4\pi}\displaystyle\int_{-\infty}^{\infty}\int_0^{2\pi} \dfrac{\varkappa_R(x_1)}{V_\infty} \times \\ \qquad \times \dfrac{(x-x_1)\cos(\psi_1-\psi)}{|\sigma|^3}\, d\psi_1\, dx_1 . \end{array} \right. \qquad (6)$$

With $\varkappa_R = \partial\Gamma_R/\partial x$, $x/R = \xi$, $\psi_1 - \psi = \pi - 2\psi$ and $k^2 = 4/[(\xi-\xi_1)^2+4]$,

Equation (6) transforms into

$$\left\{\begin{aligned}\frac{v_r(R,\xi)}{V_\infty} &= -\frac{1}{2\pi}\int_{-\infty}^{\infty}\frac{\varkappa_R(\xi_1)}{V_\infty}(\xi-\xi_1)\frac{k^3}{4}\times\\ &\times\int_0^{\pi/2}\frac{\cos 2\psi}{[(1-k^2\sin^2\psi)]^{3/2}}d\psi d\xi_1\end{aligned}\right. \tag{7}$$

or

$$\frac{v_r(R,\xi)}{V_\infty}=\frac{1}{2\pi}\int_{-\infty}^{\infty}\frac{\varkappa_R(\xi_1)}{V_\infty}(\xi-\xi_1)\frac{k^3}{4}G_1(k^2)\,d\xi_1. \tag{8}$$

The values $G_1(k^2)$ are given in tabular form in [29].

4. The cylindrical vortex surface and the manner of its deformation.

If the distribution of the vortex rings on a cylindrical surface of infinite length posesses constant strength, then from the symmetric form of Equation 8 one sees that there is no induced radial veloctiy for $\xi = 0$. With the appearance of a spatial variation in the vortex strength, an additional radial velocity arises which leads to the deformation of the vortex surfaces (Fig. 4).

For a rolled up vortex sheet of a slender wing, a sudden change in the vortex strength can occur for the following reasons (compare Fig. 5):

(a) Reduction in the strength of the departing free vortex on the leading edge of the wing through a general flow detachment in the rear region of the wing. This can also lead to a branching of the free vortex lines. The free vortex lines, which form the continuation of the bound vortex lines on the vacuum side of the wing, are coiled up in a secondary vortex sheet.

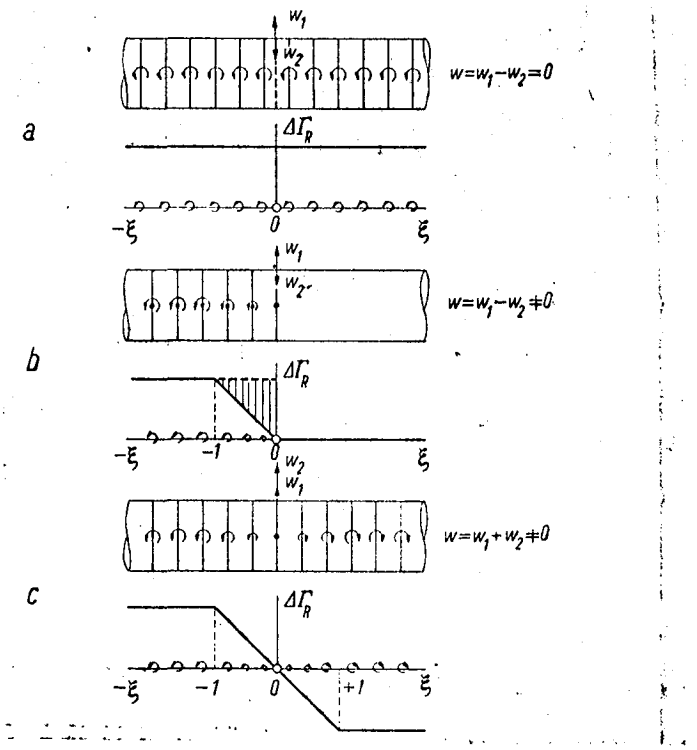

Fig. 4 The conditions for deformation of a cylindrical vortex sheet with a distribution of vortex rings.

The main vortex sheet therefore consists principally of free /359
vortices on the pressure side of the wing. This process increases substantially in the neighborhood of the trailing edge of the wing.

(b) Formation of helical vortices of opposite sense of rotation through departure of free vortices from the inner part of the wing. The free vortices, which depart downstream from the trailing edge of the wing, assume a different character with

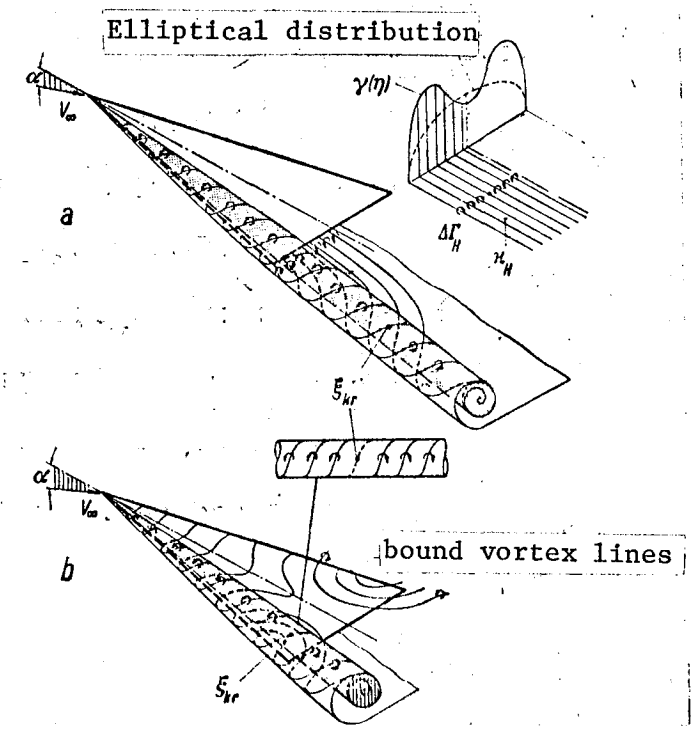

Fig. 5 Illustration of the formation of vortices of opposite sense of rotation in the cylindrical vortex sheet of a slender wing.

change in the angle of attack (Fig. 5a).

For average angles of attack, for which the circulation, $\gamma(\eta)$, of the wing detaches from the middle to the end of the wing, the free vortices from a half wing have the same rotation sense. The circulation distribtuion, $\gamma(\eta)$, becomes deformed with increasing attack anglex as illustrated in Fig. 5a. The deformation of the circulation distribution is such that a displacement of the circulation maximum takes place on both

halves of the wing. This type of circulation distribution on wings has been discussed in [24]. The declining circulation on both sides of the maximum value leads to free vortices of opposite rotation sense. Downstream, these vortices are rolled up by the large circulatory velocities of the vortex core on the ends of the wing. The position where vortices of opposite rotation sense are coiled up into the cylindrical vortex sheet is subjected to a radial induced velocity and can be designated as the critical position ξ_{crit}. If the vortex density χ_H of the departing free vortices is strong enough, a noticeable swelling of the cylindrical vortex sheet occurs at this position and to be sure, downstream from the wing. With increasing angle of attack, the vortex strength and the rolling up process become substantially greater, and consequently, the critical position wanders upstream onto the wing. This type of displacement of the critical position is known from experimental investigations.

With further increase in the angle of attack, a second type of free vortex arises on the trailing edge of the wing (Fig. 5b). For larger angles of attack, the bound vortices of a slender wing become deformed; on the inner part of the wing, they become shifted to the trailing edge of the wing as represented in Fig. 5b. For very large attack angles of the wing ($\alpha > 30°$), the bound vortices on the rear region of the inner part of the wing pass downstream, leaving the wing surfaces as free vortices and consequently become coiled into the main vortex sheet (compare Fig. 5b). Through the coiling up of both of the same vortex line, vortex lines arise on the cylindrical surface with opposite sense of rotation. Consequently, a critical position, ξ_{crit}, arises on the cylindrical surface under conditions similar to those in Fig. 5a; however, this position will be close by the wing or even over the wing surface if through the phenomenon of detachment the

bound vortices have already left the wing surface.

The local change of vortex strength of the type described does not injure the vortex propositions since each vortex line on the cylindrical surface orients itself in the resulting flow direction and subsequently arrives at the vortex core in order to continue itself downstream.

5. Determination of the swelling of a cylindrical vortex surface

Equation 8 can be applied for the mathematical determination of the deformation or change in diameter of the cylindrical surface with a distribution of ring vortices. In addition, the densities of the vortex distribution χ_W and χ_H in the free vortex sheets departing from the wing leading and trailing edges must be known. Moreover, the inclination angle, ω, of the helical vortices must be estimated in order to find out the strength of the ring vortices,

5.1 The vortex strength χ_W/V_∞

The vortex strength χ_W/V_∞ in the main vortex sheet can be derived from the following relations. The lift of the wing from the tip to the tip length x follows from

$$A(x) = \pi \varrho_\infty V_\infty^2 s^2(x)\, \bar{\alpha}(x). \qquad (9)$$

With

$$\varkappa(x) = \frac{\partial \Gamma(x)}{\partial x}, \quad \frac{\partial A}{\partial x} = \varrho V_\infty \int_{-s}^{s} \varkappa(x,y)\, dy$$

one obtains

$$\int_{-s}^{s} \varkappa(x,y)\, dy = \pi V_\infty \alpha \cdot 2 s(x) \frac{ds(x)}{dx} \qquad (10)$$

for a delta wing with constant local attack angle over the entire wing. From this one obtains for the vortex density

averaged over a stripe

$$\bar{\varkappa}(x) = \frac{1}{2s(x)} \int_{-s}^{s} \varkappa(x,y)\, dy = \pi V_\infty \alpha \frac{ds(x)}{dx}. \tag{11}$$

For the strength of the boundary vortex, the following relation is valid

$$\frac{\varkappa_W(x)}{V_\infty} = C \frac{\bar{\varkappa}(x)}{V_\infty} = C \pi \alpha \frac{ds(x)}{dx} \tag{12}$$

with $C = \chi_W/\bar{\chi}$ (compare Fig. 1).

5.2 The vortex strength χ_H/V_∞ in the free vortex sheet which is departing from the trailing edge of the wing (Fig. 5a) can be derived from the circulation distribution $\gamma(\eta)$ over the span of the wing. The following relations are valid:

$$\gamma(\eta) = \frac{c_a(\eta)\, l(\eta)}{2b} \tag{13}$$

and

$$\frac{\varkappa_H}{V_\infty} = \frac{1}{s V_\infty} \frac{\partial \Gamma}{\partial \eta} \tag{14}$$

or also

$$\frac{\varkappa_H}{V_\infty} = 2\alpha \frac{\partial}{\partial \eta} \left[\frac{c_a(\eta)\, l(\eta)}{4 s \alpha} \right] \tag{15}$$

and consequently

$$\frac{\varkappa_H}{V_\infty} = 2 \frac{\partial \gamma(\eta)}{\partial \eta}. \tag{16}$$

5.3 Estimate of the inclination angle, ω, of the vortex lines

An estimate of the inclination angle, ω, of the helical

vortex lines on the cylindrical surface will now be undertaken. The following relations are valid /360

$$\tan \omega = \frac{V_\infty + u}{v_\psi} \approx \frac{V_\infty}{v_\psi} \tag{17}$$

and

$$v_\psi = \frac{\Gamma_K}{2\pi R} + \varkappa_F \tag{18}$$

or

$$v_\psi \approx \frac{\Gamma_K}{2\pi R}. \tag{19}$$

Behind the wing, the circulation of the vortex core has the strength

$$\Gamma_K = V_\infty \int_0^l \frac{\varkappa_W}{V_\infty} dx. \tag{20}$$

For the vortex density $\chi_W/V_\infty = 1$ it follows that

$$\tan \omega = \frac{V_\infty}{v_\psi} = \frac{V_\infty}{V_\infty l} \cdot 2\pi R. \tag{21}$$

For a wing with the degree of slenderness $s/l = 1/4$ and with a characteristic diameter of the cylindrical vortex surface $2R/s = 1/3$ to $1/2$ one obtains $\tan\omega = \pi/12$ to $\pi/8$ or $\omega = 15°$ to $22°$.

Numerical values or wing data from experimental investigations of the swelling of the cylindrical surface and the collapse of the vortex core can be taken as a basis for the model calculation. For a slender delta wing with a degree of slenderness $s/l = 1/4$, the attack angle $\alpha \approx 35°$ and $C \approx 2$, the vortex density, χ_W, turns out from Equation 12 to have the value $\varkappa_W/V_\infty \approx 1$.

Consequently, from Equation 21 one obtains for the inclination angle ω

$$\frac{\varkappa_R}{V_\infty} = \frac{\varkappa_W}{V_\infty} \cos\omega \approx 1. \tag{22}$$

Further, it can be seen that for an average circulation gradient $\partial\gamma/\partial\eta = 0.5$, the vortex density χ_H assumes the value 1. This order of magnitude can be achieved on both sides of the maximal point of the deformed circultation distribution. Consequently, the value

$$\frac{\varkappa_R}{V_\infty} = \frac{\varkappa_H}{V_\infty} \cos\omega \approx \frac{\varkappa_H}{V_\infty} = 1 \tag{23}$$

for the strength of the ring vortex in the cylindrical vortex sheet can be taken as basis for the model calculation. At the critical position of the cylindrical surface, where vortices of opposite rotation sense are coiled up, the vortex strength at first diminished in both the cases of Fig. 5a and Fig. 5b; after falling to zero they again increase with opposite rotation sense.

Here it must be emphasized that the cylindrical surface only signifies a distribution surface of the ring vortices in the mathematical calculation. A similar procedure is often followed in profile theory, in which a vortex distribution is permitted to extend beyond the flow surface of the profile.

The real vortex lines continue their helical and spiral development close by this surface and arrange themselves automatically in the new flow direction which results.

That no forces arise on the free vortex sheet can be proved in the following way: the resultant velocity on the cylindrical surface reads

$$V = \sqrt{V_\infty^2 + u^2 + v_r^2 + v_\psi^2}. \tag{24}$$

Consequently, there results for the components of the forces from the ring vortex and filament vortex (compare Fig. 3)

$$\Delta K_R = -\varrho V \sin\omega \cdot \Delta\Gamma_W \cos\omega, \tag{25a}$$

$$\Delta K_F = +\varrho V \cos\omega \cdot \Delta\Gamma_W \sin\omega. \tag{25b}$$

According to this, the assumption is always fulfilled that the force on each individual free helical vortex line vanishes; i.e.

$$\Delta K_W = \Delta K_R + \Delta K_F = 0. \tag{26}$$

For the model calculation, two cases corresponding to Fig. 4b and 4c are now treated, and, to be sure, with the following development of the vortex strength (the origin of the coordinate system is placed near the area of the critical position):

Case Ia:

$$\frac{\varkappa_R(\xi_1)}{V_\infty} = \begin{cases} 1 & \text{for } \xi_1 \leqq -1, \\ -\xi_1 & \text{for } -1 < \xi_1 < 0, \\ 0 & \text{for } \xi_1 \geqq 0; \end{cases} \tag{27a}$$

Case Ib:

$$\frac{\varkappa_R(\xi_1)}{V_\infty} = \begin{cases} 1 & \text{for } \xi_1 \leqq -1, \\ -(2\xi_1 + 1) & \text{for } -1 < \xi_1 < -\frac{1}{2}, \\ 0 & \text{for } \xi_1 \geqq -\frac{1}{2}; \end{cases} \tag{27b}$$

Case II:

$$\frac{\varkappa_R(\xi_1)}{V_\infty} = \begin{cases} 1 & \text{for } \xi_1 \leqq -1, \\ -\xi_1 & \text{for } -1 < \xi_1 < +1, \\ -1 & \text{for } \xi_1 \geqq 1. \end{cases} \tag{28}$$

While case Ia and case Ib signify a linear change in the strength of the vortex rings, case II represents a linear change of vortex strength with succeeding reversal of the sense of rotation of the ring vortex.

Equation 8 is now employed to determine the induced radial velocities arising on the cylindrical vortex sheet. Since the integral exhibits a singularity for $\xi \to \xi_1$, one splits up this equation -- as in (27) -- in the following way:

$$\left\{ \begin{aligned} \frac{v_r(\xi)}{V_\infty} &= \frac{1}{2\pi} \oint_{-\infty}^{\infty} \frac{\varkappa_R(\xi_1)}{V_\infty(\xi - \xi_1)} d\xi_1 + \\ &+ \frac{1}{2\pi} \int_{-\infty}^{\infty} \frac{\varkappa_R}{V_\infty}(\xi_1)\, V_0(\xi_1)\, d\xi_1 \end{aligned} \right. \qquad (29)$$

with

$$V_0(\xi_1) = \frac{(k^3/4)\,(\xi - \xi_1)^2\, G_1(k^2) - 1}{\xi - \xi_1}. \qquad (30)$$

Now, $V_o(\xi) \to 0$ for $\xi \to \xi_1$ and, consequently, the integrand in the second integral is regular. The values $V_o(\xi_1)$ can be calculated from the values of $G_1(k^2)$ tabulated in (29). The first integral possesses a Cauchy principal value; consequently, the expression in Equation 29 is easily integrable. The integration of Equation 29 can succeed in part analytically and in part numerically.

The surface covering vortex distribution dealt with here /361
allows the vortex surface and the flow surface to deviate from each other to a certain degree. This corresponds to the theory of small deformations which is also employed in profile

theory. The deviation of the resulting flow surface from the cylindrical surface can, if necessary, be diminished by further iterations.

The results of the calculations for the cases I and II are compiled in Table 1 and depicted in Fig. 6. The swelling of the cylindrical vortex sheet for linear reduction in the strength of the ring vortex is clearly visible in Fig. 6a. A quick reduction of the vortex strength causes a sudden swelling (see case Ia and case Ib in Fig. 6a). Fig. 6b corresponds to the partial pictures 5a and 5b: a large swelling of the vortex surface arises from a reduction of the vortex strength with subsequent reversal of the rotation sense of the ring vortices. The swelling becomes considerably greater still if the reversal of the rotation sense of the ring vortex occurs in a short distance and, consequently, quickly or if the vortex strength χ_R/V_∞ increases still more.

The swelling of the cylindrical surface as well as the retardation of the flow velocity in the longitudinal direction, which are connected with the reversal of the vortex roation sense, at the same time supply the condition for the instability of the vortex core, as H. Ludwieg [22] has shown. The instability leads to the appearance of disturbance vortices and strong turbulence, which causes the vortex core to fill up the entire inner space of the already widened cylindrical surface. This process is known as breakdown of the vortex core (Fig. 7).

The critical position of the coiling of vortices of opposite rotation sense at first arises far behind the wing. With increase in the angle of attack and, consequently, the circulation strength of the vortex core, the coiling up of the free vortex sheet succeeds faster and the critical position progresses upstream.

Table I. The local inclination V_r/V_∞ of the cylindrical vortex surface with change in the vortex strength.

	Case Ia		Case Ib		Case II	
ξ	v_r/V_∞					
[1]	[1]	[°]	[1]	[°]	[1]	[°]
− 4.0	0.0041	0.2	0.0047	0.3	0.0063	0.4
− 3.0	0.0041	0.2	0.0064	0.4	0.0085	0.5
− 2.0	0.0772	4.4	0.0875	5.0	0.0885	5.1
− 1.5	0.0874	5.0	0.1119	6.4	0.1063	6.1
− 1.2	0.1229	7.0	0.1703	9.8	0.1493	8.6
− 1.1	0.1518	8.7	0.2149	12.3	0.1797	10.3
− 0.9	0.2425	13.9	0.3695	21.2	0.2817	16.1
− 0.8	0.2673	15.3	0.3972	22.8	0.3119	17.9
− 0.6	0.2890	16.6	0.3657	21.0	0.3490	20.0
− 0.4	0.2887	16.5	0.2079	11.9	0.3707	21.2
− 0.2	0.2653	15.2	0.1355	7.8	0.3772	21.6
0.0	0.1929	11.1	0.0952	5.5	0.3857	22.1
0.2	0.1169	6.7	0.0694	4.0	0.3772	21.6
0.4	0.0820	4.7	0.0520	3.0	0.3707	21.2
0.6	0.0599	3.4	0.0395	2.3	0.3490	20.0
0.8	0.0450	2.6	0.0305	1.7	0.3119	17.9
0.9	0.0393	2.3	0.0288	1.7	0.2817	16.1
1.1	0.0303	1.7	0.0215	1.2	0.1797	10.3
1.2	0.0267	1.5	0.0192	1.1	0.1493	8.6
1.5	0.0192	1.1	0.0143	0.8	0.1063	6.1
2.0	0.0112	0.6	0.0086	0.5	0.0885	5.1
3.0	0.0047	0.3	0.0039	0.2	0.0085	0.5
4.0	0.0023	0.1	0.0022	0.1	0.0063	0.4

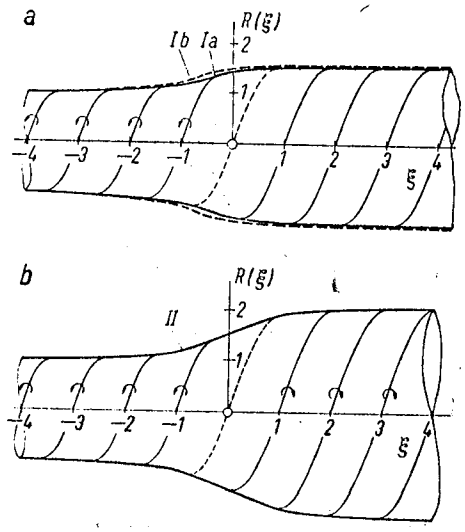

Fig. 6 The swelling of the cylindrical vortex sheet for various changes in the vortex distribution.

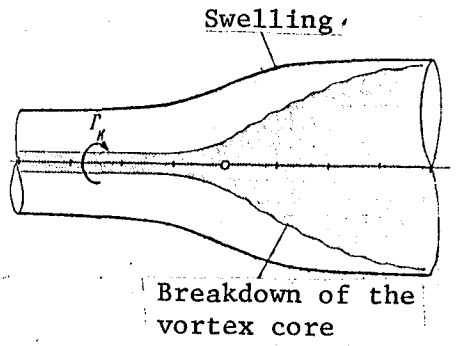

Fig. 7 Breakdown of the vortex core through instability (from [22]) in connection with the swelling of the cylindrical vortex surface.

While the retardation of the flow velocity within the rolled up vortex sheet as well as a widening of the diameter of the vortex surface appear as the primary effects of the critical position, the breakdown of the vortex core is evoked as a subsidiary phenomenon.

For constant attack angle, the circulation around a wing and, consequently, also the strength of the vortices χ_W or χ_H diminishes with increasing degree of slenderness of the wing. Consequently, for slender wings the phenomena of swelling as well as breakdown first appear for large angles of attack.

6. Summary

The rolled up vortex sheet of a slender wing with spiralling development of the vortices can be compiled from ring vortices and straight vortex filaments along a cylindrical distribution surface and a vortex core. The ring vortices contribute to the induced radial velocity which vanishes on an ∞ cylindrical vortex surface with homogeneous distribution of vortices. However, the appearance of a local change of

vortex strength or reversal of vortex rotation sense induces a radial velocity on the cylinrical surface, which leads to a deformation of the vortex surface.

From experimental observations and from the results of the theory of wings, it can be ascertained that under certain conditions a sudden reduction in vortex strength or reversal in rotation sense of the coiled vortex can appear.

The effects of such changes in strength of the ring vortex were theoretically grasped with the aid of a simplified vortex model. It can be proved that a swelling of the vortex sheet is to be expected as a consequence of the change in vortex strength or the reversal of vortex rotation sense.

With the swelling or the reversal of rotation sense of the coiled up helical vortices, the necessary condition for the instability of the vortex core and for its breakdown is supplied, as predicted by the theory of H. Ludwieg[22]. No increase in pressure in the flow direction in the field which surrounds the vortex sheet is necessary for this to occur. The condition for the breakdown is locally supplied within the coiled up sheet. These facts explain why the breakdown of the vortex core can also occur far behind the wing.

With an increase in the attack angle of the wing, the critical position, where vortices of opposite rotation sense are coiled up, progresses upstream.

The more slender a wing is, the more the swelling of the cylindrical surface or the breakdown of the vortex core is suppressed, since the strength of the ring vortex is substantially diminished with increasing degree of slenderness of the wing.

7. Literature

[1] H. Werlé: "On the vursting of turbulence at the apex of a delta wing for small velocities", La Recherche Aéronautique, Nr. 74(1960). pp 23-30

[2] A. Das: "Experiments on vortex formation in delta wings of small aspect ratio. DFL-Report Nr. 0137(1961) Compare also DFL-Report Nr. 099(1960)

[3] I.M. Hall: "Experiments with a tapered sweptback wing of Warren 12 planform at Mach numbers between 0.6 and 1.6. ARC No. 22.050(1960)

[4] M. Roy: "Remarks on the turbulent discharge around swept back wings". Z. angew. Math. Phys. 9b(1958), p. 554-569. Compare also M. Roy: "On the theory of the delta wing. Turbulence at the apex and conical sheets". La Recherche Aéronautique, No. 56(1957) p. 3-12. M. Roy: "On the formation of vortex zones in small viscosity flows". Z. Flugwiss. 7(1959) p. 217-227

[5] R. Legendre: "Conical sheets on the leading edge of a delta wing". La Renherche Aéronautique, Nr. 70(1959) p. 3-10

[6] J.H.B. Smith: "A theory of separated flow from the curved leading edges of a slender wing". ARC R & M 3116 (1959)

[7] N.C. Lambourne and D.W. Bryer: "Some measurements in the vortex flow generated by a sharp leading edge having 65° sweep". ARC No. 21.073(1959)

[8] P.T. Fink: "Wind tunnel tests on a slender wing at high incidence". Z. Flugwiss. 4(1956), S. 247-249

[9] D. Hummel: "Investigations of the breakdown of vortices for slender delta wings". Z. Flugwiss. 13(1965) p. 158-168. Compare also DFL-Report Nr. 0196(1963)

[10] D. Hummel: "Investigation on vortex breakdown on a sharp edged slender delta wing". Vortag auf dem IUTAM-Symposium on Concentrated Vortex Motions in Fluids, Ann Arbor, Mich./USA, 6-11, July 1964.

[11] B.J. Elle: "On the breakdown at high incidence of the leading edge vortices on delta wings". J. Roy. Aeron. Soc. 64(1960), S.491-493

[12] J.A. Lawford and A.R. Beauchamp: "Low speed wind tunnel measurements on a thin sharp edged delta wing with 70° leading edge sweep, with particular reference to the position of leading edge vortex breakdown". RAE TN Aero 2797(1961)

[13] J.K. Harvey: "Some observations of the vortex breakdown phenomenon. J. Fluid Mech. 14(1962), s 585-592

[14] M.V. Lowson: "Some experiments with vortex breakdown". J. Roy, Aeron. Soc. 68(1964) p. 343-346

[15] H.B. Squire: ""Analysis of the "vortex breakdown" phenomenon," Part I. Imperial College of Science and Technology, University of London, Aeron. Dept. Rep. 102(1960) Summary in: M. Schäfer (Editor), Miszellaneen der Angewandten Mechanik, ("Miscellenea of Applied Mechanics") (Festschrift Walter Tollmien). Akademie-Verlag, Berlin 1962, p. 306-312.

[16] J.P. Jone: "The breakdown of vortices in separated flow". Univeristy of Southampton, Dept. of Aeronautics and Astronautics, Re. 140(1960)

[17] M.G. Hall: "A theory of the core of a leading edge vortex". RAE Rep. Aero 2644 (1960)

[18] M.G. Hall: "On the vortex associated with flow separation from a leading edge of a slender wing". RAE TN 2629 (1959)

[19] T. Brooke-Benjamin: "Theory of the vortex breakdown phenomenon". J. Fluid. Mech. 14 (1962), p. 593-629

[20] H. Ludwieg: "Stability of the flow in a cylindrical ring space". Z. Flugwiss. 8(1960)p. 135-140. Supplement to this paper: Z. Flugwiss 9(1961) p/ 359-361

[21] H. Ludwieg: "Experimental verification of the stability theory for frictionless flows with helical streamlines" Z. Flugwiss. 12,(1964) p. 304-309

[22] H. Ludwieg: "On the explanation of the instability of free vortex cores appearing over delta wings". Z. Flugwiss. 10(1962) p 242-249

[23] H. Ludwieg: "Explanation of vortex breakdown with the help of stability theory for flows with helical streamlines". Z. Flugwiss. 13(1965) p. 437-442

[24] H. Schlichting: "Some new results on the aerodynamics of wings". Tenth Ludwig-Prandtl-memorial lecture, 1966 Yearbook of the WGLR, p 11-32

[25] H. Schlichting and E. Truckenbrodt: Aerodynamik des Flugzeug ("The Aerodynamics of the Airplane"), Vol. 1 Springer-Verlag, Berlin/Göttingen/Heidelberg, 1959

[26] O. Tietjens: Strömungslehre ("Flow Theory") Vol. 1 Springer-Verlag, Berlin/Göttingen/Heidelberg, 1960.

[27] J. Weissinger: "On the aerodynamics of the ringwing in incompressible flow". Z. Flugwiss. 4(1956) p. 141-150

[28] D. Küchemann and J. Weber: "Aerodynamics of Propulsion. McGraw-Hill Book Company, New York, London 1953

[29] F. Riegels: "The flow around fast rotation symmetric bodies". Communications of the Max Planck Institute for Flow Research Nr. 5 (1952)